

Anomalous dip observed in intensity autocorrelation function as an inherent nature of single-photon emitters

H. Nakajima,^{1,2, a)} H. Kumano,¹ H. Iijima,¹ and I. Suemune¹

¹⁾*Research Institute for Electronic Science, Hokkaido University, Sapporo 001-0021, Japan*

²⁾*Research Fellow of the Japan Society for the Promotion of Science, Tokyo 102-8472, Japan*

(Dated: 30 July 2012)

We report the observation of an anomalous antibunching dip in intensity autocorrelation function with photon correlation measurements on a single-photon emitter (SPE). We show that the anomalous dip observed is a manifestation of quantum nature of SPEs. Taking population dynamics in a quantum two-level system into account correctly, we redefine intensity autocorrelation function. This is of primary importance for precisely evaluating the lowest-level probability of multiphoton generation in SPEs toward realizing versatile pure SPEs for quantum information and communication.

^{a)}Electronic mail: nakajima@es.hokudai.ac.jp

A variety of single-photon emitters (SPEs)^{1–20} have been widely investigated for applications in quantum key distribution (QKD)²¹, quantum information processing²², and quantum metrology²³. Single-photon emission has been demonstrated by using quantum two-level systems formed in single molecules^{1,2}, atoms^{3,4}, ions⁵, color centers in diamond^{6–8}, and semiconductor quantum dots (QDs)^{9–20}. Generating single-photon pure state is crucial for assuring the firm security in the cryptography²⁴ and also minimizing error rate in linear optical quantum computing²⁵. Therefore, suppression of the multiphoton generation is strongly required for the practical SPEs. Recently, with a variety of quantum systems, SPEs with considerably low multiphoton probability have been reported^{4,12,14}, and implementation to the prototype QKD systems has also been demonstrated^{6,13,15}.

Photons generated from SPEs are generally inspected with the Hanbury-Brown and Twiss (HBT) setup²⁶, where photons separated into two arms are introduced to single-photon detectors located on each arm for photon correlation measurements. The intensity autocorrelation function²⁷ is composed of coincidence counts as a function of the delay time τ between photon detection events in each detector. The coincidence counts at $\tau = 0$ exhibit a simultaneous photon detection by the two detectors. Therefore, multiphoton generation can be directly measured with coincidence counts at $\tau = 0$ ^{1,7–11} and this usually appears as a *peak* in the intensity autocorrelation function.

In this paper, observation of counterintuitive *dip*-shaped structure at $\tau \sim 0$ in intensity autocorrelation function is reported for the first time. We show the dip structure originates from an inherent nature of a single quantum emitter. In order to explicitly include population dynamics in a quantum two-level system, we derive an extended form of the conventionally used intensity autocorrelation function. This provides a way to precisely determine the probability of generating single-photon pure states from SPEs over a wide range of operating conditions.

InAs QDs grown on (001) GaAs by metalorganic molecular-beam epitaxy was used to realize a SPE. For isolating a single QD, pillar structures with the diameter of 500 nm were formed with reactive ion etching and were embedded with metal to enhance photon extraction efficiency. Further details on sample preparation are given in refs. 17 and 18. Optical properties of the QDs were examined by a standard micro-photoluminescence (μ -PL) setup equipped with a mode-locked Ti:sapphire laser (photon energy of 1.3920 eV, pulse repetition period of 13.2 ns, pulse duration of ~ 5 ps) and a Si charge-coupled-device detector. Figure 1 (a) shows a μ -PL spectrum observed from a single QD at 20 K. The excitation power was $2.1 \mu\text{W}$ which corresponds to the average number of excitons (\bar{N}_X) photoinjected into the QD of ~ 0.2 . The emission line centered

at 1.3214 eV is prominent and we focus on this line hereafter. From the linear excitation power dependence of the PL intensity and the presence of finite exciton fine structure splitting²⁸, this emission line was assigned to be a neutral exciton (X^0).

Under the same excitation condition, a photon correlation measurement was carried out with the HBT setup employing a pair of single-photon counting modules (SPCMs). Resultant intensity autocorrelation function is displayed as black line in Fig. 1 (b) with its expanded view around zero delay in the lower trace. The accumulation time for building up the histogram with a multi-channel scaler was about 10 h. Strongly suppressed coincidence counts at $\tau \sim 0$ manifest highly pure single-photon emission from the present SPE.

Here, we analyze the measured intensity autocorrelation function with a commonly accepted formula under nonresonant pulsed excitation^{6,7,10,18,19}

$$N^{-1} \left\{ B + \alpha_0 \exp\left(-\frac{|\tau|}{\tau_e}\right) + \sum_{n \neq 0} \alpha_n \exp\left(-\frac{|\tau - n \cdot T_{rep}|}{\tau_e}\right) \right\}, \quad (1)$$

where α_0 , $\alpha_{n(\neq 0)}$, T_{rep} , τ_e and N are the degree of multiphoton contribution ($0 \leq \alpha_0 \leq 1$), correlation peak height of n -th excitation cycle ($\alpha_{n(\neq 0)} \equiv 1$), repetition period of the excitation pulses, decay time constant of the emitter, and the normalization factor, respectively.

Here, B is the baseline originating from an accidental coincidence, estimated to be ~ 0.009 ²⁹. As for τ_e , we have independently measured the decay profile of the X^0 emission line (inset of Fig. 1 (a)), and obtained double-exponential decay times of 0.9 and 6.1 ns. The shorter decay component is the exciton lifetime commonly observed in InAs QDs¹⁶, while the longer one is most probably due to additional transitions involving other excitonic states, such as dark excitons³⁰ or charged excitons³¹. Intensity autocorrelation function based on Eq. (1) is simulated³² and the convoluted result with a system response function is displayed as the green dashed line in Fig. 1 (b). In this simulation, α_0 was set to zero assuming an ideal SPE. The overall properties are well reproduced. However, the important finding is that the measured coincidence counts at $\tau \sim 0$ are lower than the one calculated with Eq. (1) for the ideal SPE, which yields an anomalous dip rather than usually observed peak at $\tau = 0$. This is, to the best of our knowledge, the first observation of the anomalous dip structure in the intensity autocorrelation function for SPEs.

The observed dip-shaped coincidence with a cusp at $\tau = 0$ reveals that there exists qualitative difference between the measured intensity autocorrelation function and Eq. (1). We discuss, to clarify the difference, the coincidence counts between photons labeled as the first and second photons triggered by the different excitation pulses. Assuming for simplicity that excitation pulse

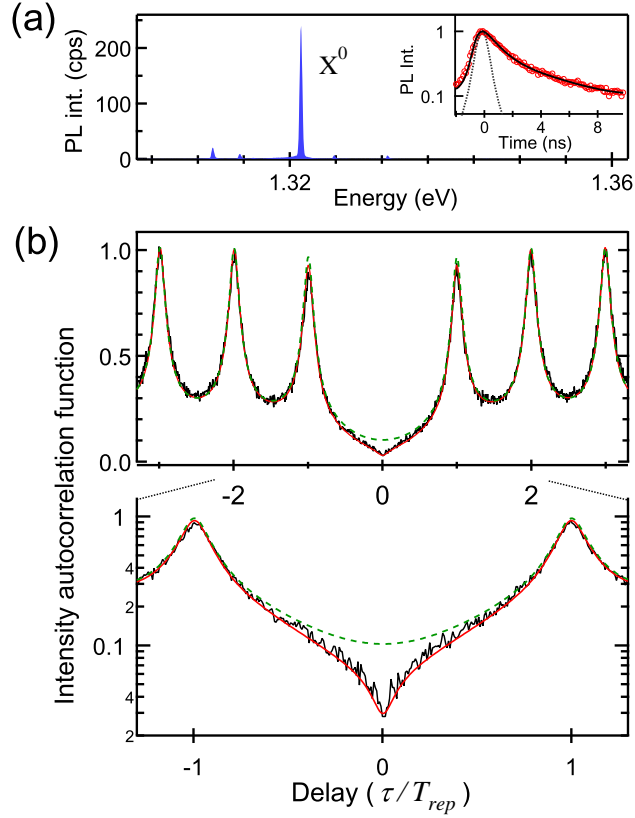


FIG. 1. (a) μ -PL spectrum from a single InAs QD. Inset indicates a decay profile of the X^0 emission line (red circles) and fitted result (black line) convoluted with a response function of our whole system (dotted line). (b) Measured intensity autocorrelation function (black line) for the X^0 emission line with a time bin of 100 ps. Simulated curves based on Eq. (1) with $\alpha_0 = 0$ (green dashed line) and Eq. (2) (red line) are also shown. Both curves are convoluted with a system response function. Measured autocorrelation function has a cusp at $\tau = 0$, which is not consistent with Eq. (1). The red curve indicates the best fit to the measured function, which gives $\alpha_0 = 0.003$. Expanded view at $\tau \sim 0$ in a logarithmic scale is displayed at the bottom.

drives the exciton population in a QD, $p_{|X\rangle}$, to unity and the second photons are emitted instantaneously after excitation at $t = T_{rep}$ (Fig. 2). The $p_{|X\rangle}$ initiated to unity at $t = 0$ will relax to the ground state (GS) with decay time constant of τ_e as indicated by the green line in Fig. 2. The coincidence between the first and second photons indicated by the black arrow occurs at the delay time of $\tau = T_{rep} - t_0$, and its counts are proportional to $\exp(-t_0/\tau_e)$, which is the exciton population at the time of the first photon emission. Provided that the exciton populated at $t = 0$ decays independently of the next excitation at $t = T_{rep}$, the coincidence counts could be recorded even

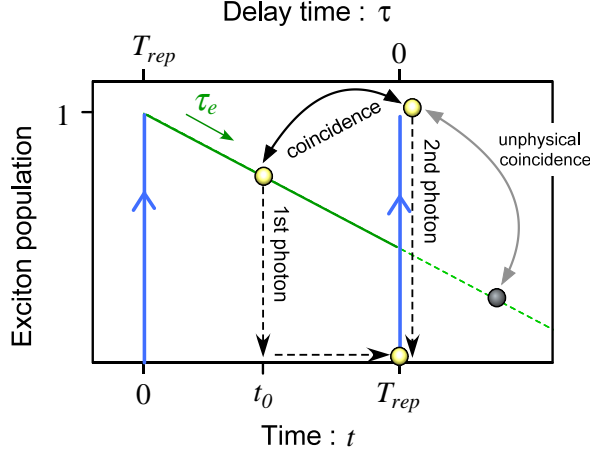


FIG. 2. Schematic of the dynamics of exciton population in a QD. Green thin line indicates the decay profile of exciton populated at $t = 0$ as a function of t (bottom axis) and delay time τ with respect to $t = T_{rep}$ (upper axis). After the first photon emission at t_0 , system stays in the ground state until next excitation (black dashed arrow). Black arrow indicates possible coincidence between the first and second photon emissions, while the gray arrow corresponds to unphysical coincidence in which the exciton decay is independent of the subsequent excitations as reflected in Eq. (1).

for $t \geq T_{rep}$ ($\tau \leq 0$) as shown in the gray arrow. The conventional formula Eq. (1) is formulated under this situation, in which all the contribution of the photon pairs to the coincidence counts is summed up uncorrelatedly to the population dynamics which takes place in the excitation and emission processes (green dashed curve in Fig. 1(b)). In a realistic quantum two-level system, in contrast, once the first photon is emitted at the time t_0 ($0 \leq t_0 \leq T_{rep}$), the population in a QD is reset to the GS and keeps in the GS until experiencing the next excitation at $t = T_{rep}$ as displayed by the black dashed arrow in Fig. 2. Therefore, no coincidence count is possible for $\tau \leq 0$. This gives rise to the essential difference between observed intensity autocorrelation function and Eq. (1).

The population decay for $\tau \leq 0$ which brings unphysical coincidence counts is expressed by $\exp(-|\tau|/\tau_e)$ (green dashed line) with its amplitude being normalized by the exciton population at $\tau = 0$. Since the sum of population probability over two states in the quantum two-level system is unity for arbitrary delay time of τ , physically valid coincidence is given by the complementary counterpart of the unphysical coincidence, i.e., $1 - \exp(-|\tau|/\tau_e)$. This term corresponds to the modulation intensity to apply to the unphysical coincidence counts given at each delay time of

τ in Eq. (1), so that the quantum nature of the emitter as a two-level system is appropriately incorporated into the intensity autocorrelation function. This is the brief interpretation to the observed anomalous dip structure with a cusp at zero delay.

According to the above argument, we define an extended intensity autocorrelation function including the population dynamics in a quantum two-level system as

$$\tilde{g}^{(2)}(\tau \geq 0) = N^{-1} \left\{ B + \alpha_0 \exp\left(-\frac{|\tau|}{\tau_e}\right) + \sum_{n>0} \alpha_n \exp\left(-\frac{|\tau - n \cdot T_{rep}|}{\tau_e}\right) \cdot [1 - \exp(-|\tau|/\tau_e)] \right\}, \quad (2)$$

and $\tilde{g}^{(2)}(\tau \leq 0) = \tilde{g}^{(2)}(-\tau)^{33}$. In comparison to Eq. (1), the anomalous dip observed at $\tau \sim 0$ is satisfactorily reproduced with the $\tilde{g}^{(2)}(\tau)$ as indicated by the red line in Fig. 1 (b). Furthermore, the extended function allows us to precisely determine the multiphoton contribution of $\alpha_0 = 0.003$ which cannot be derived with Eq. (1). These results demonstrate that considering the population dynamics, as an inherent nature of quantum emitters, is essential for evaluating the intensity autocorrelation function under the pulsed excitation.

In what follows, we discuss the condition for emerging the anomalous antibunching dip based on Eq. (2). The anomalous dip is caused by applying the modulation term $1 - \exp(-\tau/\tau_e)$ to unphysical coincidence counts characterized by exciton population at $t = T_{rep}$, i.e., $\exp(-T_{rep}/\tau_e)$ (see Fig. 2 and Eq. (1)). Thus, for evaluating the α_0 , it is beneficial to describe the dip depth as a function of T_{rep}/τ_e which is specified by selecting the emitter and the repetition period of the excitation. Here, we introduce the dip depth defined by $\Delta - \tilde{g}^{(2)}(0) = \Delta - \alpha_0$, where Δ is the lower limit of the coincidence counts at $\tau = 0$ without considering the inherent nature of quantum emitter³⁴, and we set $B = 0$. Figure 3 presents the calculated dip depth as a function of T_{rep}/τ_e for some α_0 values. In this figure, all traces tend to $-\alpha_0$ for sufficiently high T_{rep}/τ_e , which indicates that peak-shaped coincidence with the amplitude of α_0 appears as the multiphoton contribution. In this condition, Eq. (2) reduces to Eq. (1). Actually, in most of reports, α_0 has been evaluated with relatively high T_{rep}/τ_e region such as $> 10^{1,5,7,9,10,13}$. However, for the low T_{rep}/τ_e region, dip-shaped coincidence emerges. This is because the coincidence counts based on the uncorrelated decay (green dashed line in Fig. 2) are overestimated, and the amplitude of modulation required to include the quantum nature is enhanced for the low T_{rep}/τ_e . Thus, the conventional formula Eq. (1) is no longer valid. In the present case, since $T_{rep}/\tau_e \sim 2.2$ and $\Delta > \alpha_0$, the anomalous dip was clearly observed as indicated by Fig. 1 (b). Therefore, it is essential to employ the $\tilde{g}^{(2)}(\tau)$ especially for the SPEs with low α_0 operating with low T_{rep}/τ_e conditions such as high repetition cycles.^{19,20}

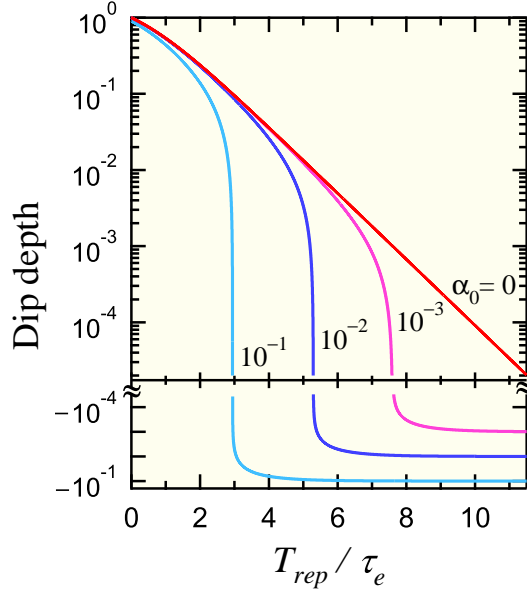


FIG. 3. Calculated depth of anomalous dip at $\tau = 0$ as a function of T_{rep}/τ_e for specific α_0 values. In this calculation, $B = 0$ is assumed and system response function is not taken into account. Negative value represents peak-shaped coincidence at $\tau \sim 0$. The dip structure will be distinct for SPEs with low α_0 operating with low T_{rep}/τ_e conditions. For sufficiently high T_{rep}/τ_e , the dip depth approaches to $-\alpha_0$. Generalized intensity autocorrelation function presented in this work is applicable to the whole T_{rep}/τ_e range, which is essential to precisely evaluate the α_0 under arbitrary operating conditions.

Note that the fine fitting for the height of each correlation peak at $\tau = n \cdot T_{rep}$ ($|n| \geq 1$) shown in Fig. 2 is due to relatively low excitation condition such that $\bar{N}_X \sim 0.2$. For larger excitation power, the peak heights are subject to the effect of excitation rate of G as is the case with the well-known antibunching lineshape in a single-photon emission under cw excitation.³⁵ On the other hand, the derived modulation term $1 - \exp(-|\tau|/\tau_e)$ is irrelevant to the G for $\tau \sim 0$ since the system is free from excitation.

In conclusion, we have reported the observation of an anomalous antibunching dip in intensity autocorrelation function with a semiconductor single-photon emitter. By redefining the autocorrelation function to include the population dynamics in quantum emitters, the observed dip was clearly interpreted. Applying the extended autocorrelation function to the result of the photon correlation measurements enables us to successfully evaluate one of the most important figure of merit α_0 even with relatively low T_{rep}/τ_e condition evoking a dip at around zero delay. Our find-

ings are invaluable to deal with versatile single-photon emitters demanded for the state-of-the-art quantum information devices.

The authors would like to acknowledge Dr. H. Sasakura and Dr. C. Hermannstädter for fruitful discussions. This work was supported in part by the Grant-in-Aid for Scientific Research (B), No.24310084, (S), No.24226007, Hokkaido Innovation Through Nanotechnology Supports (HINTs) from the Ministry of Education, Culture, Sports, Science and Technology, and Strategic Information and Communications R&D Promotion Programme (SCOPE) from Ministry of Internal Affairs and Communications.

REFERENCES

- ¹B. Lounis, and W. E. Moerner, *Nature* **407**, 491 (2000).
- ²M. Nothaft, S. Höhla, F. Jelezko, N. Fruhauf, J. Pflaum, and J. Wrachtrup, *Nat. Commu.* **3**, 628 (2012).
- ³A. Kuhn, M. Hennrich, and G. Rempe, *Phys. Rev. Lett.* **89**, 067901 (2002).
- ⁴B. Darquié, M. P. A. Jones, J. Dingjan, J. Beugnon, S. Bergamini, Y. Sotais, G. Messin, A. Browaeys, and P. Grangier, *Science* **309**, 454 (2005).
- ⁵M. Keller, B. Lange, K. Hayasaka, W. Lange, and H. Walther, *Nature* **431**, 1075 (2004).
- ⁶A. Beveratos, R. Brouri, T. Gacoin, A. Villing, J.-Ph. Poizat, and P. Grangier, *Phys. Rev. Lett.* **89**, 187901 (2002).
- ⁷K. Y. Han, K. I. Willig, E. Rittweger, F. Jelezko, C. Eggeling, and S. W. Hell, *Nano Letters* **9**, 3323 (2009).
- ⁸B. J. M. Hausmann, T. M. Babinec, J. T. Choy, J. S. Hodges, S. Hong, I. Bulu, A. Yacoby, M. D. Lukin, and M. Lončar, *New Journal of Physics* **13**, 045004 (2011).
- ⁹P. Michler, A. Kiraz, C. Becher, W. V. Schoenfeld, P. M. Petroff, L. Zhang, E. Hu, and A. Imamoglu, *Science* **290**, 2282 (2000).
- ¹⁰V. Zwiller, H. Blom, P. Jonsson, N. Panev, S. Jeppesen, T. Tsegaye, E. Goobar, M.-E. Pistol, L. Samuelson, and G. Bjork, *Appl. Phys. Lett.* **78**, 2476 (2001).
- ¹¹M. Pelton, C. Santori, J. Vučković, B. Zhang, G. S. Solomon, J. Plant, and Y. Yamamoto, *Phys. Rev. Lett.* **89**, 233602 (2002).
- ¹²P. Ester, L. Lackmann, S. Michaelisde Vasconcellos, M. C. Hübner, and A. Zrenner, *Appl. Phys. Lett.* **91**, 111110 (2007).

- ¹³K. Takemoto, Y. Nambu, T. Miyazawa, K. Wakui, S. Hirose, T. Usuki, M. Takatsu, N. Yokoyama, K. Yoshino, A. Tomita, S. Yoroazu, Y. Sakuma, and Y. Arakawa, *Applied Physics Express* **3**, 092802 (2010).
- ¹⁴J. Claudon, J. Bleuse, N. S. Malik, M. Bazin, P. Jaffrennou, N. Gregersen, C. Sauvan, P. Lalanne, and J.-M. Gérard, *Nat. Photon.* **4**, 174 (2010).
- ¹⁵P. M. Intallura, M. B. Ward, O. Z. Karimov, Z.L. Yuan, P. See, A. J. Shields, P. Atkinson, and D. A. Ritchie, *Appl. Phys. Lett.* **91**, 161103 (2007).
- ¹⁶C. Becher, A. Kiraz, P. Michler, A. Immamoğlu, W. V. Schoenfeld, P. M. Petroff, L. Zhang, and E. Hu, *Phys. Rev. B* **63**, 121312 (2001).
- ¹⁷H. Kumano, H. Nakajima, S. Ekuni, Y. Idutsu, H. Sasakura, and I. Suemune, *Advances in Mathematical Physics* **2010**, 1 (2010).
- ¹⁸H. Nakajima, S. Ekuni, H. Kumano, Y. Idutsu, S. Miyamura, D. Kato, S. Ida, H. Sasakura, and I. Suemune, *physica status solidi (c)* **8**, 337 (2011).
- ¹⁹K. Rivoire, S. Buchley, A. Majumdar, H. Kim, P. Petroff, and J. Vučković, *Appl. Phys. Lett.* **98**, 083105 (2011).
- ²⁰A. Lochmann, E. Stock, J. A. Töflinger, W. Unrau, A. Toropov, A. Bakarov, V. Haisler, and D. Bimberg, *Electron. Lett.* **45**, 566 (2009).
- ²¹N. Gisin, G. Ribordy, W. Tittel, and H. Zbinden, *Reviews of Modern Physics* **74**, 145 (2002).
- ²²M. A. Nielsen and I. L. Chuang, eds., *Quantum Computation and Quantum Information* (Cambridge University Press, Cambridge, 2000).
- ²³V. Giovannetti, S. Lloyd, and L. Maccone, *Nat. Photon.* **5**, 222 (2011).
- ²⁴E. Waks, C. Santori, and Y. Yamamoto, *Phys. Rev. A* **66**, 042315 (2002).
- ²⁵E. Knill, R. Laflamme, and G. J. Milburn, *Nature* **409**, 46 (2001).
- ²⁶R. H. Brown and R. Q. Twiss, *Nature* **177**, 27 (1956).
- ²⁷R. J. Glauber, *Phys. Rev.* **130**, 2529 (1963).
- ²⁸M. Bayer, G. Ortner, O. Stern, A. Kuther, A. A. Gorbunov, A. Forchel, P. Hawrylak, S. Fafard, K. Hinzer, T. L. Reinecke, S. N. Walck, J. P. Reithmaier, F. Kloppe, and F. Schäfer, *Phys. Rev. B* **65**, 195315 (2002).
- ²⁹Fraction of accidental coincidence count for emitters under cw excitation is estimated by $(2SD + D^2)/(S + D)^2$, where S and D are measured signal and dark count rates, respectively (ref. 16). In our case, S (D) was approximately 11,500 (120) counts/s, leading to $(2SD + D^2)/(S + D)^2 \sim 0.021$. The baseline B for pulsed operation is given by the fraction of accidental coincidence

count in time-averaged coincidence counts per pixel in a multi-channel scaler (MCS). Thus B is obtained by normalized coincidence counts of 814.5 integrated over a relatively wide time bin of 184.8 ns (1848 MCS pixels) as $814.5/1848 \times 0.021$.

³⁰P. A. Dalgarno, J. M. Smith, B. D. Gerardot, A. O. Govorov, K. Karrai, P. M. Petroff, and R. J. Warburton, *physica status solidi (a)* **202**, 2591 (2005).

³¹B. Piechal, J. Suffczynski, A. Trajnerowicz, M. Goryca, P. Kossacki, A. Golnik, and J. Gaj, *Acta Physica Polonica A* **108**, 831 (2005).

³²The emitter employed in this work shows double-exponential decay, thus the term $\exp(-1/\tau_e)$ in Eq. (1) can be rewritten as $A_1 \exp(-1/\tau_1) + A_2 \exp(-1/\tau_2)$, where A_1, A_2, τ_1, τ_2 are 0.69, 0.31, 0.9 ns, 6.1 ns, respectively.

³³In the redefined intensity autocorrelation function, symmetrization operation to be even function in terms of τ is carried out after summing up all the contribution of physically possible coincidence counts triggered by excitations for $n > 0$.

³⁴Function value of Eq. (1) at $\tau = 0$ corresponds to Δ with $\alpha_0 = B = 0$. Using Σ defined as $2 \cdot \sum_{n>0} \alpha_n \exp(-n \cdot T_{rep}/\tau_e)$, we have $\Delta = \Sigma/(1 + \Sigma)$.

³⁵B. Lounis, H.A. Bechtel, D. Gerion, P. Alivisatos, and W.E. Moerner, *Chemical Physics Letters* **329**, 399 (2000).